Effects of spin-orbit coupling on quantum transport
Bardarson, J.H.

Chapter 1

Introduction

In the center of Leiden there is a little park alongside a tranquil canal. On the other side of the canal, facing the park, is a magnificent old building that radiates history. The first hint towards its nature is the towering name *Kamerlingh Onnes* that marks the buildings front face[1]. This is, of course, the old physics building of the University of Leiden. Many great minds have graced this place with their presence and one of them, Paul Ehrenfest[2], has a particularly strong influence on this thesis. This influence, as we will discuss shortly, is both direct and indirect through three of his students: Hendrik Anthony Kramers, George Uhlenbeck, and Samuel Goudsmit (Fig. 1.1).

A few words about the contents of this thesis are, before revealing the connection to Ehrenfest, in order. The word *effects* in the title, hints at a certain diversity in the topics covered. In fact, in later chapters we will be concerned with a number of seemingly unrelated topics including quantum

---

[1]Heike Kamerlingh Onnes received the Nobel Prize in Physics in 1913 "for his investigations on the properties of matter at low temperatures which led, inter alia, to the production of liquid helium". He discovered superconductivity with his student Holst [1].

[2]It is fitting that it is Ehrenfest that takes the central stage in this story, for he was a genuine scientist. Einstein supposedly said that "he was not merely the best teacher in our profession whom I have ever known; he was also passionately preoccupied with the development and destiny of men, especially his students. To understand others, to gain their friendship and trust, to aid anyone embroiled in outer or inner struggles, to encourage youthful talent – all this was his real element, almost more than his immersion in scientific problems".
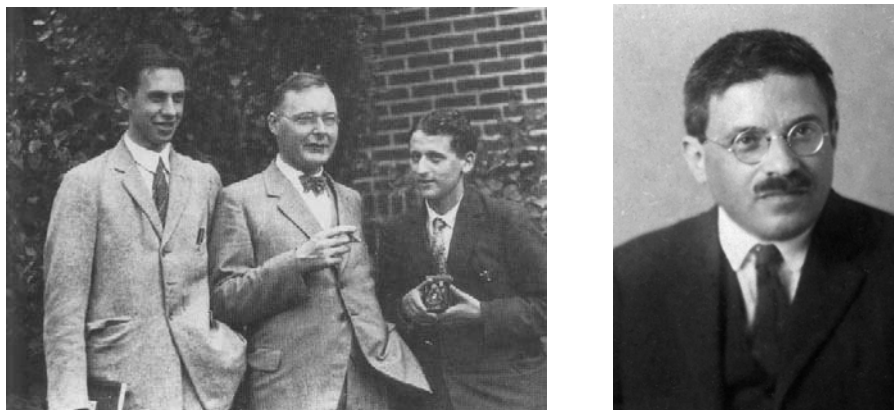
Figure 1.1. Left panel: The inventors of spin, George Uhlenbeck (left) and Samuel Goudsmit (right), with Hendrik Kramers who first noticed a twofold degeneracy in the solutions to the Schrödinger equation with spin: the Kramers degeneracy. All three were students of Paul Ehrenfest (right panel) in Leiden.

chaos, electronic shot noise, electron-hole entanglement, spin Hall effect, and (absence of) Anderson localization. While it certainly would be useful to have an extensive introduction to all these different topics there simply is not enough space to do them all justice (a brief introduction is given in Sec. 1.4). Instead, in this introduction, the focus is on what brings all these topics together in this thesis, namely *spin-orbit coupling*. In particular, we will concentrate on some fundamental aspects of quantum transport in the presence of spin-orbit coupling, the details of which are assumed known in the literature but are not always easily found in textbooks.

Before going into details, it is unavoidable in a thesis so involved with spin, to mention *spintronics*; if only as a means of motivation. Spintronics is a large field whose name indicates the wish to do electronics with spins. There are several technological reasons why one would want to do that, and initial successes are a testimony to their validity. Let us, however, not go down that road, but rather view the word spintronics as denoting the drive towards a fundamental understanding of quantum transport of spins. With this view it is difficult, for a physicist, not to get excited. The spin has from its discovery by Uhlenbeck and Goudsmit (under the guidance of

Ehrenfest[3]) tickled the imagination of physicists. Being purely quantum mechanical some of its properties are plain puzzling, but it is the simplicity of its description coupled with the richness of its physics that excites.

But let us not get too carried away, we were talking about spintronics. Initially, much of the interest was in systems that combined ferromagnets with metals or semiconductors. Later, interest grew in purely electronic systems, in which one talks to the spin degree of freedom through spin-orbit coupling. In this thesis we will be concerned with the latter type of systems.

To set the stage we will in this introduction start by giving a general introduction to spin and spin-orbit coupling in Sec. 1.1. Spin-orbit coupling conserves time reversal symmetry. The consequences of time reversal have thus to be taken into account. One particularly important consequence is a degeneracy named after the third of Ehrenfest students, the *Kramers degeneracy*. (We have now mentioned all the indirect influences of Ehrenfest, his direct influence will be encountered in chapter 3 on the effect of spin-orbit coupling on the Ehrenfest time[4].) In Sec. 1.2 we give a detailed account of time reversal symmetry and its consequences for the spectrum and symmetries of Hamiltonians and scattering matrices.

In Sec. 1.3 we solve two model Hamiltonians, the Rashba Hamiltonian and the single valley graphene Dirac Hamiltonian, whose solutions will be useful in later chapters. Finally, in Sec. 1.4 we give a brief introduction to each of the chapters of this thesis.

1.1 Spin and Spin-Orbit Coupling

It was after a detailed study of spectroscopic data that Uhlenbeck and Goudsmit came to suggest that the electron has spin, an intrinsic angular

---

[3]Ehrenfest's contribution, allowing his students to go ahead with a wild idea with the words "you are both young enough to be able to afford a stupidity", was crucial. About the same time, Ralph Kronig had similar ideas, but the response of his supervisor, Wolfgang Pauli, "it is indeed very clever but of course has nothing to do with reality", was in stark contrast to Ehrenfest's.

[4]Strictly speaking, the Ehrenfest time does not come directly from Ehrenfest himself. The Ehrenfest time τ_E is the time it takes a wavepacket to spread to a size on the order of the system size. For times smaller then τ_E the center of the wavepacket and its group velocity satisfy Ehrenfest's theorem, thus the name.

momentum that gives arise to a magnetic moment. Most physicists first acquaintance with spin, however, is through a recount of the Stern-Gerlach experiment [2]. Building on this familiarity, we will begin our discussion by using a combination of the results of the experiment and classical arguments to deduce the presence of the spin and a coupling of this spin to the orbital motion. The same results are then obtained more rigorously from the nonrelativistic limit of the Dirac equation. In turn, this leads us to an analysis of the rotation properties of spin and the accompanying Berry phase. We demonstrate the importance of this phase by considering its role in weak (anti) localization. To complete this section, we sketch how the spin-orbit coupling in semiconductors gives rise to the familiar Rashba and Dresselhaus terms.

1.1.1   Spin and the Stern-Gerlach Experiment

With their experiment, Stern and Gerlach, established the following empirical fact: The electron has an intrinsic magnetic moment $\boldsymbol{\mu}_s$ which takes on quantized values $\pm\mu_B$ along any axis ($\mu_B = e\hbar/2mc$ is the Bohr magneton). This suggests the introduction of a quantum number $\sigma = \pm$ such that the wavefunction of the electron can be represented by a two component spinor

$$\psi(\boldsymbol{r}) = \begin{pmatrix} \psi_+(\boldsymbol{r}) \\ \psi_-(\boldsymbol{r}) \end{pmatrix}. \tag{1.1}$$

Quite often the state of the electron factorizes, i.e. it can be written as a direct product $|\psi\rangle \otimes |\chi\rangle$ where $|\chi\rangle$ is a state vector (two component spinor) in the two dimensional Hilbert space of the spin. Any operator in this two dimensional space (i.e. any 2×2 matrix[5]) can be written as a linear combination of the 2×2 unit matrix $\mathbb{1}$ and the *Pauli matrices*

$$\sigma_1 = \begin{pmatrix} 0 & 1 \\ 1 & 0 \end{pmatrix}, \quad \sigma_2 = \begin{pmatrix} 0 & -i \\ i & 0 \end{pmatrix}, \quad \sigma_3 = \begin{pmatrix} 1 & 0 \\ 0 & -1 \end{pmatrix}. \tag{1.2}$$

In particular, any vector operator is necessarily proportional to $\boldsymbol{\sigma} = (\sigma_1, \sigma_2, \sigma_3)$.

What are the consequences of this empirical fact? Suppose our electron

---

[5]See also the section 1.2.2 on quaternions.

is moving with velocity $\boldsymbol{v}$ in an electric field $-e\boldsymbol{E} = -\boldsymbol{\nabla}V$. Classically the magnetic moment does not couple to the electric field. However, taking into account relativistic effects, the electron sees in its rest frame a magnetic field, which to order $(v/c)^2$ (with c the speed of light) is given by $\boldsymbol{B} = -\boldsymbol{v} \times \boldsymbol{E}/c$ [3]. The interaction of the magnetic moment $\boldsymbol{\mu}_s$ with this magnetic field leads to a potential energy term

$$V_{\mu_s} = -\boldsymbol{\mu}_s \cdot \boldsymbol{B} = \boldsymbol{\mu}_s \cdot \frac{\boldsymbol{v}}{c} \times \boldsymbol{E} = \frac{1}{ec}\boldsymbol{\mu}_s \cdot \boldsymbol{v} \times \boldsymbol{\nabla}V. \qquad (1.3)$$

In an atom, the potential giving rise to the electric field is central $V = V(r)$ and

$$V_{\mu_s} = \frac{1}{ecr}\frac{dV}{dr}\boldsymbol{\mu}_s \cdot \boldsymbol{v} \times \boldsymbol{r} = -\frac{1}{emcr}\boldsymbol{\mu}_s \cdot \boldsymbol{L}, \qquad (1.4)$$

with $\boldsymbol{L} = \boldsymbol{r} \times \boldsymbol{p}$ the orbital angular momentum and m the electron mass. Including this term in the quantum description, the conservation of angular momentum seems to be broken (since the components of $\boldsymbol{L}$ do not commute). To rescue the conservation of angular momentum, the electron needs to have an intrinsic angular momentum $\boldsymbol{S}$. In analogy with orbital moments, we expect the magnetic moment $\boldsymbol{\mu}_s$ to be proportional to the angular momentum

$$\boldsymbol{\mu}_s = -\frac{g_s\mu_B}{\hbar}\boldsymbol{S}. \qquad (1.5)$$

Since $\boldsymbol{S}$ is a vector operator in spin space it is necessarily a multiple of $\boldsymbol{\sigma}$. The interaction term V_{μ_s} is thus proportional to $\boldsymbol{\sigma} \cdot \boldsymbol{L}$. The only possible choice for $\boldsymbol{S}$ such that the full angular momentum $\boldsymbol{J} = \boldsymbol{L} + \boldsymbol{S}$ is conserved turns out to be [2]

$$\boldsymbol{S} = \frac{\hbar}{2}\boldsymbol{\sigma}. \qquad (1.6)$$

The magnetic moment becomes $\boldsymbol{\mu}_s = -(g_s/2)\mu_B\boldsymbol{\sigma}$ and since the eigenvalues of the Pauli matrices are ± 1 we need to take the g factor $g_s = 2$ to explain the observed quantization of $\boldsymbol{\mu}$.

With a careful consideration of their experiment we have learned a lot from Stern and Gerlach. We have been able to deduce the existence of the spin and we have seen how the interaction of the magnetic moment with

the electric field can alternatively be seen as a spin-orbit coupling

$$V_{\mu_s} = \frac{\hbar}{2m^2c^2}\frac{1}{r}\frac{dV}{dr}\boldsymbol{\sigma}\cdot\boldsymbol{L},\tag{1.7}$$

In a noncentral potential this spin-orbit coupling is

$$V_{\mu_s} = -\frac{\hbar}{2m^2c^2}\boldsymbol{\sigma}\cdot\boldsymbol{p}\times\nabla V.\tag{1.8}$$

This is still not the full story. In addition to the effect just described we need to take into account a term that has a purely kinematic origin. To be able to use the above results we need to be in the rest frame of the electron. Since the electron is accelerating the reference frame is constantly changing. This amounts to successive Lorentz boosts. However since Lorentz boosts do not form a subgroup in the group of Lorentz transformations (which includes boosts and rotations) two successive boosts are in general not equivalent to another boost but rather to a boost followed by a rotation. There is thus an additional precession, *Thomas precession*, that needs to be taken into account. This turns out to give a contribution of the same form as (1.8) but with opposite sign and half the amplitude [3]. The full spin-orbit coupling term is thus

$$V_{\text{so}} = -\frac{\hbar}{4m^2c^2}\boldsymbol{\sigma}\cdot\boldsymbol{p}\times\nabla V.\tag{1.9}$$

1.1.2   Spin-Orbit Coupling from the Dirac Equation

Last section painted a nice physical picture of the origin of spin-orbit coupling. The arguments, however, are a bit handwavy and alternate between being classical, quantum and relativistic. A more satisfactory, albeit less physically transparent, derivation can be obtained by taking the nonrelativistic limit of the Dirac equation. This procedure leads to the Pauli equation. In this section we sketch the derivation following the more general derivation given by Sakurai [4].

In the standard representation, and in Hamiltonian form, the Dirac

equation is $H \left| \psi \right\rangle = E \left| \psi \right\rangle$ with [4]

$$H = \begin{pmatrix} 0 & c \, \boldsymbol{p} \cdot \boldsymbol{\sigma} \\ c \, \boldsymbol{p} \cdot \boldsymbol{\sigma} & 0 \end{pmatrix} + \begin{pmatrix} mc^2 & 0 \\ 0 & -mc^2 \end{pmatrix}. \tag{1.10}$$

Writing $\left| \psi \right\rangle = (\psi_A, \psi_B)^T$ we have two coupled equations for ψ_A and ψ_B. Using the second equation to eliminated ψ_B we obtain

$$\boldsymbol{p} \cdot \boldsymbol{\sigma} \frac{c^2}{E + mc^2} \boldsymbol{p} \cdot \boldsymbol{\sigma} \psi_A = (E - mc^2) \psi_A. \tag{1.11}$$

In the presence of a potential V, we make the substitution $E \rightarrow E - V$. We are interested in the nonrelativistic limit, so we write $E = mc^2 + \epsilon$ with $\epsilon \ll mc^2$. Further assuming that $|V| \ll mc^2$ we can expand

$$\frac{c^2}{E - V + mc^2} = \frac{1}{2m} \left(1 - \frac{\epsilon - V}{2mc^2} + \cdots \right). \tag{1.12}$$

Since $mv^2/2 + V \sim \epsilon$, the second term is seen to be of order $(v/c)^2$. To zeroth order, using[6] $(\boldsymbol{p} \cdot \boldsymbol{\sigma})(\boldsymbol{p} \cdot \boldsymbol{\sigma}) = p^2$, we simply obtain the Schrödinger equation

$$\left(\frac{p^2}{2m} + V \right) \psi = \epsilon \psi. \tag{1.13}$$

The reason this derivation works is that to zeroth order in (v/c), $\psi_B = 0$. In fact, from (1.10) we have to first order in $(v/c)^2$

$$\psi_B = \frac{\boldsymbol{p} \cdot \boldsymbol{\sigma}}{2mc} \psi_A. \tag{1.14}$$

In other words, in this limit ψ_A is equivalent to the Schrödinger wave-function ψ. When going to next order, more care must be taken. The probabilistic interpretation of Dirac theory requires the normalization

$$\int (\psi_A^\dagger \psi_A + \psi_B^\dagger \psi_B) = 1. \tag{1.15}$$

---

[6] As a special case of the more general formula $(\boldsymbol{\sigma} \cdot \boldsymbol{A})(\boldsymbol{\sigma} \cdot \boldsymbol{B}) = \boldsymbol{A} \cdot \boldsymbol{B} + i\boldsymbol{\sigma} \cdot (\boldsymbol{A} \times \boldsymbol{B})$.

To first order, using (1.14), this gives

$$\int \psi_A^\dagger \left(1 + \frac{p^2}{4m^2c^2} \right) \psi_A = 1. \tag{1.16}$$

Apparently, to have a normalized wave function, we should use $\psi = [1 + p^2/(8m^2c^2)]\psi_A$. Substituting this into the Dirac equation, and using the expansion (1.12), we obtain after some rearrangement [4] the Pauli equation

$$\left(\frac{p^2}{2m} + V - \frac{p^4}{8m^3c^2} - \frac{\hbar}{4m^2c^2}\boldsymbol{\sigma} \cdot \boldsymbol{p} \times \boldsymbol{\nabla}V + \frac{\hbar^2}{8m^2c^2}\boldsymbol{\nabla}^2 V \right) \psi = \epsilon\psi. \tag{1.17}$$

All the terms in this equation have a ready made interpretation. The third term is simply a relativistic correction to the kinetic energy, and the last term gives a shift in energy. The fourth term is the spin-orbit coupling term (1.9) we derived heuristically in the last section. It is gratifying to obtain the same result from the Dirac equation.

1.1.3   Spin and Rotations

Not only does the spin-orbit coupling emerge naturally from the Dirac equation, the spin itself is buried within the equation. Recall that the Dirac equation can be obtained with little more then Lorentz invariance. To discuss how spin arises in the Dirac equation we need to briefly discuss the theory of rotations. Since we will learn important facts about the rotations of spins at the same time, it is a worthwhile endeavor.

Infinitesimal rotations in a three dimensional space, of an angle $\delta\varphi$ about an axis $\hat{\boldsymbol{n}}$, are given by

$$U_R = \mathbb{1} - \frac{i}{\hbar}\delta\varphi\,\hat{\boldsymbol{n}} \cdot \boldsymbol{J}, \tag{1.18}$$

with $\boldsymbol{J} = (J_x, J_y, J_z)$ three operators which are called the *generators of infinitesimal rotations*. From the properties of rotations one deduces that the components of $\boldsymbol{J}$ satisfy the commutation relations [2]

$$[J_i, J_j] = i\hbar\varepsilon_{ijk}J_k, \tag{1.19}$$

with ε_{ijk} the fully antisymmetric tensor, or Levi-Civita symbol[7]. These are just the commutation relations of an angular momentum. In particular, rotations of a spin half particles are given by (1.18) with $\boldsymbol{J} = \boldsymbol{S}$. Integrating (1.18) and using the relation (1.6) of $\boldsymbol{S}$ to $\boldsymbol{\sigma}$, finite rotations of spin are given by

$$U_s = \exp\left(-i\frac{\varphi}{2}\hat{\boldsymbol{n}} \cdot \boldsymbol{\sigma}\right) = \cos\frac{\varphi}{2} - i\hat{\boldsymbol{n}} \cdot \boldsymbol{\sigma}\sin\frac{\varphi}{2}. \qquad (1.20)$$

To obtain the second equality, we used that[8] $(\hat{\boldsymbol{n}} \cdot \boldsymbol{\sigma})^2 = 1$. As a consequence, we notice that a rotation of 2π does not bring you back to the same state, but rather minus the state, i.e. $U_s(2\pi) = -1$.

On first acquaintance this minus sign is odd. The mathematical explanation, that SU(2) is a twofold covering of SO(3), is only illuminating once you know what it means. Physicists like to picture the spin as living on the Bloch sphere. This description, however, does not contain the Berry's phase since a rotation of 2π brings you back to the same point on the Bloch sphere. The reason, of course, is that in constructing the Bloch sphere, a global phase factor of a general spin state was ignored. For an isolated spin this global phase factor does not lead to any observable effect, but there are cases when it is important (see below).

One way to picture what is going on, is to introduce a "Möbius-Bloch sphere"[9]. To explain what that means, start by picturing the normal Möbius strip, embedded in three dimensional space. Imagine walking along the strip with a cap on your head carrying an arrow that points upwards. Now you walk along the strip and after walking half of the strip, you are back at the same point in the three dimensional embedding space. In this space, however, you are on the "other side" of the strip, your arrow pointing in the opposite direction[10] (minus sign). If you were to identify the point you are on now, with the point that you started from, you would have a circle and you find you have gone around the full circle. But if you do not identify the point you find that you need to walk another full circle

---

[7]$\varepsilon_{ijk} = 1(-1)$ for an (odd) even permutation of (123) and zero otherwise.

[8]A consequence of the relation in footnote 6 and $|\hat{\boldsymbol{n}}|^2 = 1$.

[9]We are not aware of a strict mathematical equivalence between SU(2) and a "Möbius-Bloch sphere". It is introduced here for ease of visualization.

[10]Other side within quotations marks, since the Möbius strip has only one side.

to come back to your original point of departure. Generalizing this to the sphere, you imagine any great circle on the sphere to be a Möbius strip, and the fact that rotation about 2π gives a minus sign can be visualized[11].

How does spin come about in the Dirac equation? As already mentioned the Dirac equation is constructed to be Lorentz invariant. In demanding this invariance, in particular one can consider infinitesimal rotations. One finds that for the Dirac equation to be invariant the Dirac spinors need to transform in a certain way. Equating this transformation with general statement (1.18) about angular momentum as generators of rotation, one can simply read of the angular momentum of the electron. In addition to the orbital angular momentum $\boldsymbol{L}$ one indeed finds an intrinsic angular momentum[12] given by $\boldsymbol{S} = \hbar/2\boldsymbol{\sigma}$ as we had concluded earlier from the Stern-Gerlach experiment.

We conclude this section with an example of the effect of the (Berry's) phase obtained from a rotation of the spin. The effect we consider is the weak (anti)localization [5], which is a quantum correction to the classical conductance of a system arising from quantum interference. To understand the effect, imagine injecting a particle into a scattering region and ask about the probability for it to return. Let us start with the spinless case. The probability amplitude of reflection back in the same mode can be written as a sum over classical paths γ starting and ending at the same point [6]

$$r = \sum_{\gamma} \mathcal{A}_{\gamma} \exp\left(\frac{i}{\hbar}\mathcal{S}_{\gamma}\right). \tag{1.21}$$

$\mathcal{S}_{\gamma}$ is the action along γ and $\mathcal{A}_{\gamma}$ is a classical weight. The reflection probability is

$$R = rr^{\dagger} = \sum_{\gamma,\gamma'} \mathcal{A}_{\gamma}\mathcal{A}_{\gamma'}^{*}e^{i/\hbar(\mathcal{S}_{\gamma}-\mathcal{S}_{\gamma'})}. \tag{1.22}$$

In the classical limit, $\hbar \to 0$, the exponential is quickly oscillating, and

---

[11]Incidentally, your shoulder has the same property. Imagine holding a cup filled with coffee in one hand. Now rotate it by an angle 2π without spilling it. You find that to obtain that goal you needed to twist your arm which is now inverted (it acquired a "minus sign"). With some skill you can rotate the cup another 2π in the same direction, to find yourself in your initial configuration.

[12]Or more exactly, an angular momentum that in the nonrelativistic limit reduces to the Pauli equation spin [4].
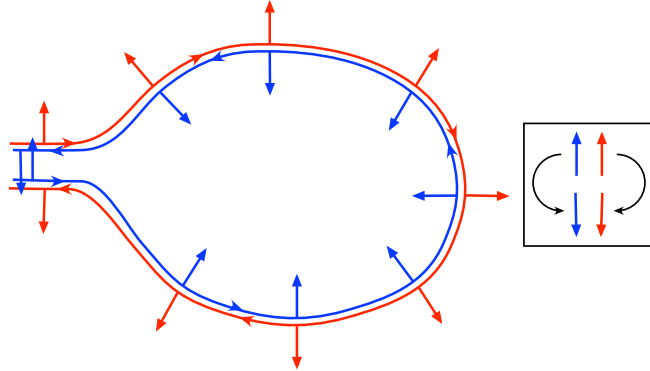
Figure 1.2. A schematic representation of a trajectory (red) and it time reverse (blue). The spin dynamics are assumed adiabatic such that the spin just adjusts itself to be always in an eigenstate. As the (time reversed) trajectory is followed the spin is seen to rotate about an angle of π $(-\pi)$. This rotation of the spin leads to an extra phase causing a destructive interference between the two paths.

only the paths with $S_\gamma = S_{\gamma'}$ contribute to the sum. In particular, the classical reflection probability is obtained by including only the terms with $\gamma' = \gamma$,

$$R_{\mathrm{cl}} = \sum_\gamma |\mathcal{A}_\gamma|^2. \tag{1.23}$$

In the presence of time reversal symmetry, the time reversed path $\tilde{\gamma}$ has the same action and weight factor as γ. Thus, in addition to the classical contribution, we have the extra term

$$R_{\mathrm{wl}} = \sum_{\gamma=\tilde{\gamma}} |\mathcal{A}_\gamma|^2 = R_{\mathrm{cl}}. \tag{1.24}$$

We thus see that the total reflection probability $R = R_{\mathrm{cl}} + R_{\mathrm{wl}} = 2R_{\mathrm{cl}}$ is enhanced compared to the classical reflection probability. This leads to a smaller conductance, and the correction term is referred to as *weak localization*. Essentially the path γ and its time reverse $\tilde{\gamma}$ interfere constructively to enhance the reflection probability.

When we have spin-orbit coupling there is more to the story. Most of the time the spin-orbit coupling is weak, so we can ignore the effect it has

on trajectories. The spin-orbit coupling does however rotate the spin of the electron as it moves around the classical path. One then finds that the only modification to the reflection amplitude r, is an introduction of a spin phase factor [7, 8] K_γ

$$r = \sum_\gamma K_\gamma \mathcal{A}_\gamma \exp\left(\frac{i}{\hbar}\mathcal{S}_\gamma\right). \qquad (1.25)$$

The reflection probability becomes

$$R = rr^\dagger = \sum_{\gamma,\gamma'} \mathcal{M}_{\gamma,\gamma'} \mathcal{A}_\gamma \mathcal{A}_{\gamma'}^* e^{i/\hbar(\mathcal{S}_\gamma - \mathcal{S}_{\gamma'})}. \qquad (1.26)$$

with $\mathcal{M}_{\gamma,\gamma'} = K_\gamma K_{\gamma'}^*$ a *spin modulation factor*. K_γ is essentially[13] just $e^{i\alpha_\gamma}$ with α_γ the phase picked up by rotating the spin as we go along the path γ. Therefore, $\mathcal{M}_{\gamma,\gamma} = 1$ and the classical contribution to the reflection amplitude $R_{\rm cl}$ is the same as in the spinless case. If the spin-orbit coupling is strong enough the spin will simply adiabatically follow the path. The contribution of the time reversed pair of paths gets an extra minus sign $\mathcal{M}_{\gamma,\tilde\gamma} = -1$. The reason is that following the path γ the spin is rotated by π, while for the path $\tilde\gamma$ it is rotated by $-\pi$ (see Fig. 1.2). Because of the complex conjugation in $\mathcal{M}_{\gamma,\tilde\gamma} = K_\gamma K_{\tilde\gamma}^*$ these two phases add up to give a total rotation of 2π, leading to a Berry's phase of -1. The quantum correction

$$R_{\rm wal} = \sum_{\gamma=\tilde\gamma} \mathcal{M}_{\gamma,\tilde\gamma} |\mathcal{A}_\gamma|^2 = -R_{\rm cl}, \qquad (1.27)$$

is referred to as *weak antilocalization*. The total reflection amplitude $R = R_{\rm cl} + R_{\rm wal} = 0$ vanishes, leading to a larger conductance.

Note that there is of course some reflection. What we considered here was only a part of the full scattering problem, namely we only looked at reflection back into the same mode.[14] This is why in the full problem (when

---

[13]We are simplifying things a bit here, K_γ is really matrix elements of a propagator of spin dynamics, and $\mathcal{M}$ is the trace over a product of propagators [7, 8]. The essential physics is still contained in our presentation.

[14]Actually, if the incident mode was $|n\rangle$ we looked at reflection into its time reverse

taking into account all modes), the classical contribution is proportional to the number of modes N, while the weak (anti)localization correction is of order one.

1.1.4 Spin-Orbit Coupling in Semiconductors

The Pauli equation (1.17) describes an electron moving in vacuum in the presence of a potential V. In a single particle picture of a solid, essentially the same equation can be used to obtain effective Hamiltonians describing the movement of electrons. Usually, we neglect the third and fifth term and write

$$\left(\frac{p^2}{2m} + V_0(\boldsymbol{r}) - \frac{\hbar}{4m^2 c^2} \boldsymbol{\sigma} \cdot \boldsymbol{p} \times \boldsymbol{\nabla} V_0 + V(\boldsymbol{r}) \right) \psi = E\psi. \qquad (1.28)$$

Here V_0 is the periodic crystal potential, and V is an external applied potential (e.g. gate voltage). The main contribution to the spin-orbit coupling comes from the crystal potential, so we have neglected V in the third term.

We are interested in obtaining an effective Hamiltonian describing the motion of electrons in our semiconductor. There are essentially two approaches. One is the theory of invariants which is a purely group theoretical approach. The second, the Kane model, tries to obtain a solution with reasonable approximation to Eq. (1.28). It is the second approach we want to discuss here. A detailed account has been given of the method and the calculations in Refs. 9 and 10, to which we refer for details. Fortunately, we only need to introduce a few energy scales to get a flavor of the derivation and the meaning of its results.

In the absence of the spin-orbit term and external potentials a solution of Eq. (1.28) gives us the first approximation to the bandstructure of the solid. In the semiconductors we have in mind, the part of the bandstructure we are interested in will consist of a conduction band and a valence band separated by a band gap E_0 at a certain k value. Often (e.g. in GaAs) this is the Γ point $k = 0$. One can understand these bands as emerging from

---

$T \left| n \right\rangle$. In the spinless case, this is simply reversal of momentum, in the spin case the direction of the spin is also inverted (cf. Sec. 1.2.5).

the atomic levels of the constituent atoms of the solid. The conduction band is derived from s orbitals of the atom (basis states $|S\rangle$) and the valence band from p orbitals (basis states $|X\rangle , |Y\rangle , |Z\rangle$). The conduction band is therefore twofold (because of spin) and the valence band sixfold degenerate at the band edge (Γ point).

When we take into account the spin-orbit coupling, the bands become mixed and are now characterized by their total angular momentum quantum numbers (j and m_j) plus the orbital momentum index $l = 0$ ($l = 1$) characterizing the conduction (valence) bands. The conduction band now has $j = 1/2$ and $m_j = \pm 1/2$ while two of the valence bands ($j = 1/2, m_j = \pm 1/2$) split off from the other four ($j = 3/2, m_j = \pm 1/2, \pm 3/2$). In addition the $j = 3/2$ bands, while degenerate at the band edge, have a different curvature (i.e. effective mass) and are referred to as heavy hole (hh) and light hole (lh) band (cf. Fig. 1.3). The split off energy Δ_0 is simply given by an energy scale obtained from the spin-orbit coupling term

$$\Delta_0 = -\frac{3i\hbar}{4m^2c^2}\langle X|(\boldsymbol{\nabla} V_0 \times \boldsymbol{p}) \cdot \hat{\boldsymbol{y}}|Z\rangle. \tag{1.29}$$

The basic idea of the Kane model is that the band edge eigenstates (eigenstates with a fixed k) constitute a complete basis. To obtain the eigenstates away from the band edge we simply expand the wavefunction (in an envelope function approximation) in the band edge states. Bands that are far away in energy can be neglected. In the original Kane model, only the bands in Fig. 1.3 where taken into account, leading to an 8×8 band Hamiltonian

$$H = \begin{pmatrix} H_{cc} & H_{cv} \\ H_{vc} & H_{vv} \end{pmatrix}. \tag{1.30}$$

Here H_{cc} (H_{vv}) is the block of the conduction (valence) band eigenstates. The coupling H_{cv} between the conduction and valence band depends on the momentum operator matrix element

$$P_0 = \frac{\hbar}{m}\langle S|p_x|X\rangle. \tag{1.31}$$

Once one has the Hamiltonian (1.30), the final step is to find a unitary
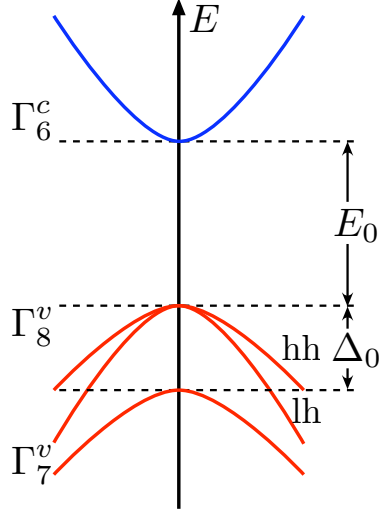
Figure 1.3. A schematic of the band structure of a zinc-blend structure, showing the twofold conduction band (Γ_6^c) and the six spin-orbit split valence bands (Γ_7^v and Γ_8^v). The conduction band and the topmost valence bands (heavy hole (hh) and light hole (lh)) are separated by the energy gap E_0. The spin-orbit split off valence band (Γ_7^v) is separated from the other valence bands by the energy Δ_0.

transformation U such that

$$UHU^\dagger = \begin{pmatrix} \tilde{H}_{cc} & 0 \\ 0 & \tilde{H}_{vv} \end{pmatrix}, \tag{1.32}$$

where $\tilde{H}_{cc}$ is now our effective Hamiltonian describing electrons in the conduction band.

Instead of going through the details, let us simply discuss the results of such a procedure, focusing on the spin-orbit coupling terms (the leading order terms will simply be the usual kinetic energy term with an effective mass). In a perturbation theory around $\boldsymbol{k} = 0$ we expect the lowest order terms that couple to the spin to be linear in $\boldsymbol{k}$. We can write

$$H_{\text{so}} = -\boldsymbol{B}(\boldsymbol{k}) \cdot \boldsymbol{\sigma}. \tag{1.33}$$

Time reversal symmetry requires $\boldsymbol{B}(-\boldsymbol{k}) = -\boldsymbol{B}(\boldsymbol{k})$. If in addition the

system has an inversion symmetry $\boldsymbol{B}(-\boldsymbol{k}) = \boldsymbol{B}(\boldsymbol{k})$ and the only possible solution is $\boldsymbol{B}(\boldsymbol{k}) = 0$. Thus for the term (1.33) to be nonzero the inversion symmetry needs to be broken[15].

In heterostructures the confinement potential and the band edge variations (different materials have different band gaps etc.) break the inversion symmetry. Taking this into account the procedure described above leads to the Rashba term

$$H_R = \alpha(k_x\sigma_y - k_y\sigma_x) \tag{1.34}$$

where

$$\alpha = \langle\alpha(z)\rangle, \tag{1.35a}$$

$$\alpha(z) = \frac{P_0^2}{3}\left[\frac{1}{(E_0 + \Delta_0)^2} - \frac{1}{E_0^2}\right]\frac{dV}{dz}, \tag{1.35b}$$

with $\langle\ \rangle$ denoting an average over the z subband eigenstate that confines the electron to form a two dimensional electron gas.

A couple of important features of the Rashba spin-orbit coupling can be seen from the expression (1.35) for α. First is that it depends on the external (gate) potential V. We thus see that the size of α can be tuned by playing with the gate voltages. Second, we observe that the presence of Rashba spin-orbit coupling relies crucially on the size of the spin-orbit coupling in the semiconductor (as measured by Δ_0). If $\Delta_0 = 0$, $\alpha = 0$ regardless of the strength of the external potential. It is really by traveling near the nuclei that the electron picks up most of the spin-orbit coupling.

In zinc blend structure, such as GaAs, the inversion symmetry is also broken in the bulk leading to the Dresselhaus term

$$H_D = \beta(k_x\sigma_x - k_y\sigma_y). \tag{1.36}$$

To obtain this term one needs to take into account higher conduction bands so the expression for β is more complicated and contains additional parameters we have not defined, so we skip writing it down. In addition to

---

[15]Or time reversal symmetry which is trivially done by applying a magnetic field. We are interested in the all electronic setups (no magnetic fields) so we do not consider this possibility.

the linear Dresselhaus term (1.36) there is also a cubic (in k) Dresselhaus term which can be of importance [9].

1.2   Time Reversal and Kramers Degeneracy

In 1930 H. A. Kramers in his study of the Schrödinger equation of an electron with spin in the absence of a magnetic field, found a mapping T that given a solution $|\psi\rangle$ with energy E gives another solution $T|\psi\rangle$ with the same energy [11]. For systems with odd number of spin half electrons these solutions are orthogonal and therefore lead to a degeneracy in the spectrum, the *Kramers degeneracy*. A couple of years later Wigner pointed out that the mapping Kramers found is simply time reversal and that the degeneracy is a manifestation of the presence of time reversal symmetry [12].

Symmetries in quantum mechanics can be represented either by unitary and linear operators or antiunitary and antilinear operators, according to a theorem also due to Wigner [13]. We will see that time reversal is necessarily in the latter, somewhat less familiar category. There is a crucial difference between the two groups in the fact that while unitary symmetries lead to a conserved quantity (e.g. translation symmetry to conservation of momentum and rotation symmetry to conservation of angular momentum) antiunitary symmetries in general do not. The effect of antiunitary symmetries (time reversal) is thus more subtle, as reflected in the Kramers degeneracy, but just as important.

In addition to the Kramers degeneracy of energy eigenvalues, the presence of time reversal imposes a symmetry on Hamiltonians and scattering matrices. Furthermore, in scattering, transmission eigenvalues are twofold degenerate. The exact symmetries of the Hamiltonian are usually given in terms of quaternions (or Pauli sigma matrices) in which they take a simple form.

All the above mentioned properties are of importance in any quantum theory of transport. In the literature, these have become a common knowledge and are used as such. For a newcomer, it can take some time to dig up definitions and proofs of these important properties, in particular since topics such as antiunitary operators and quaternions are often not

included in textbooks. In the case of the Kramers degeneracy of transmission eigenvalues, the proofs that exist in the literature are somewhat convoluted and not given directly in terms of the scattering matrix. In this section we therefore represent definitions and proofs in a unified manner, and an alternative proof of the Kramers degeneracy of transmission eigenvalues.

We start by a review of the mathematical concepts of antiunitary operators and quaternions. Time reversal is then explained and its consequences for Hamiltonians and scattering matrices explored.

1.2.1 Antiunitary Operators

An operator T is said to be *antilinear*, if for any state vectors $|\varphi\rangle$, $|\psi\rangle$ and complex numbers α, β, it satisfies

$$T(\alpha\,|\varphi\rangle + \beta\,|\psi\rangle) = \alpha^* T\,|\varphi\rangle + \beta^* T\,|\psi\rangle. \qquad (1.37)$$

The asterisk denotes complex conjugation. If in addition T has the property

$$|\langle\psi|\varphi\rangle| = |\langle T\psi|T\varphi\rangle|, \qquad (1.38)$$

it is called *antiunitary* [13]. The relations (1.37) and (1.38) lead to the equality[16]

$$\langle T\psi|\,T\varphi\rangle = \langle\psi|\,\varphi\rangle^*, \qquad (1.39)$$

which can equivalently be taken as the definition of antiunitarity [15].

The operator $\mathcal{C}$ of complex conjugation (with respect to the (orthogonal) basis $\{|n\rangle\}$) is an antiunitary operator that satisfies

$$\mathcal{C}\,|n\rangle = |n\rangle \quad \forall n, \quad \text{and} \quad \mathcal{C}^2 = 1. \qquad (1.40)$$

---

[16]Note that the use of Dirac bra-ket notation, developed for *linear* vector spaces, is a risky business when dealing with antilinear operators. The safest approach is to let T first act on a ket, and only then use the dual correspondence to find the corresponding bra [14].

The action of $\mathcal{C}$ on a general state vector

$$|\psi\rangle = \sum_n c_n |n\rangle \qquad (1.41)$$

is completely determined by these properties

$$\mathcal{C} |\psi\rangle = \sum_n c_n^* |n\rangle . \qquad (1.42)$$

In particular, if

$$|\varphi\rangle = \sum_n d_n |n\rangle \qquad (1.43)$$

we can confirm the antiunitary property (1.39)

$$\langle \mathcal{C}\psi | \mathcal{C}\varphi \rangle = \sum_n c_n d_n^* = \langle \psi | \varphi \rangle^*. \qquad (1.44)$$

A product of an antiunitary and a unitary operator is again antiunitary, while the product of two antiunitary operators is unitary. Every antiunitary operator T can therefore be written as a product of a unitary operator U and the complex conjugation operator $\mathcal{C}$ (the form of U will depend on the basis with respect to which $\mathcal{C}$ is defined)

$$T = U\mathcal{C}. \qquad (1.45)$$

In particular, the time reversal operator, our prime example of an antiunitary symmetry (and the reason for using here the symbol T to represent an antiunitary operator), will always be written in this form.

1.2.2   Quaternions

Sir W. R. Hamilton introduced quaternions as a generalization of complex numbers. Walking with his wife along the Royal Canal in Dublin, the defining equations of quaternions

$$\boldsymbol{i}^2 = \boldsymbol{j}^2 = \boldsymbol{k}^2 = \boldsymbol{ijk} = -1 \qquad (1.46)$$

came to him in a burst of inspiration. In his excitement he carved them into stone at the Brougham Bridge [16]. The story does not elaborate on what his wife was doing meanwhile.

One of the consequences of the defining equation (1.46) is that the basic quaternions $\boldsymbol{i}, \boldsymbol{j}, \boldsymbol{k}$ do not commute. There are different representations of the algebraic structure of quaternions, the most common being in terms of the Pauli matrices (1.2) (see below).

Hamilton spent much of the rest of his life trying to realize the usefulness and beauty of complex numbers in his quaternions. There are strong reasons why that cannot work[17], and thus he was not very successful. So why do we want to use quaternions? For us, the main reason, perhaps, is bookkeeping. The Hamiltonian in a basis which is a direct product of a real space state vector and a two dimensional spin state vector, has a natural decomposition into blocks of 2×2 matrices, which can then be thought of as a single quaternion. Instead of taking the Hamiltonian to be a $2N \times 2N$ complex matrix, one can consider it to be an $N \times N$ matrix of quaternions. What does one gain by doing this? Mainly an economic way of expressing symmetry relations and performing calculations[18].

With this motivation in mind we are ready to dive into the mathematical definitions of quaternions. A quaternion is defined as a linear combination of the 2×2 unit matrix $\mathbb{1}$ and the Pauli spin matrices[19] (1.2) [18]

$$q = q_0 \mathbb{1} + i\boldsymbol{q} \cdot \boldsymbol{\sigma}, \tag{1.47}$$

with $\boldsymbol{q} = (q_1, q_2, q_3)$ a vector of complex numbers, and $\boldsymbol{\sigma} = (\sigma_1, \sigma_2, \sigma_3)$. The *quaternionic complex conjugate*[20] $\tilde{q}$ and *hermitian conjugate* $q^\dagger$ are

---

[17]For example, the concept of an analytical function has no counterpart.

[18]In random matrix theory calculations, for example, averages over the symplectic ensemble written in terms of quaternions can be translated into averages over the orthogonal ensemble [17].

[19]To make the connection to Hamiltons defining equation (1.46) we note the connection $\boldsymbol{i} = i\sigma_3$, $\boldsymbol{j} = i\sigma_2$ and $\boldsymbol{k} = i\sigma_1$.

[20]This notation is not standard. Most of the time people denote the quaternionic complex conjugate simply with an asterisk. Since the quaternionic complex conjugate differs from the normal complex conjugate, and we will mostly use the latter, we adopt a different notation to avoid confusion.

defined as

$$\tilde{q} = q_0^* + i\boldsymbol{q}^* \cdot \boldsymbol{\sigma} = \sigma_2 q^* \sigma_2, \qquad (1.48a)$$

$$q^\dagger = q_0^* - i\boldsymbol{q}^* \boldsymbol{\sigma}. \qquad (1.48b)$$

A quaternion is called real if $\tilde{q} = q$. We define the *dual* of a quaternion[21] with

$$q^R = q_0 - i\boldsymbol{q} \cdot \boldsymbol{\sigma} = \sigma_2 q^T \sigma_2. \qquad (1.49)$$

For completeness, we mention that the trace of a quaternion is $\operatorname{tr} q = q_0$ (half the normal trace).

The quaternionic complex (hermitian) conjugate $\tilde{Q}$ ($Q^\dagger$) of a quaternionic matrix is the (transpose of the) matrix of the quaternionic complex (hermitian) conjugates

$$(\tilde{Q})_{ij} = \widetilde{(Q_{ij})}, \qquad (1.50a)$$

$$(Q^\dagger)_{ij} = (Q_{ji})^\dagger. \qquad (1.50b)$$

The dual of a quaternionic matrix $Q^R = (\tilde{Q})^\dagger$. A matrix which equals its dual, is called self-dual. For a hermitian matrix, self-dual and quaternionic real are equivalent. The trace of a quaternionic matrix is $\sum_j \operatorname{tr} Q_{jj}$.

1.2.3 Time Reversal

Having covered some mathematical ground, let us now turn our attention to time reversal symmetry (which we will sometimes refer to as $\mathcal{T}$-symmetry). In some sense, it is better to think of time reversal as being reversal of motion rather than actual reversal of time. The conventional time reversal of a spinless particle reverses its momentum but the position is unchanged.

Let us make this a little bit more abstract by considering Fig. 1.4. We imagine following a path in Hilbert space parameterized by time t. The evolution from state $|\psi(t)\rangle$ to $|\psi(t')\rangle$ is given by the time evolution operator $U(t', t) = \exp[-iH(t' - t)/\hbar]$. The arrows help us remember the

---

[21]Sometimes called *conjugate quaternion* [18].
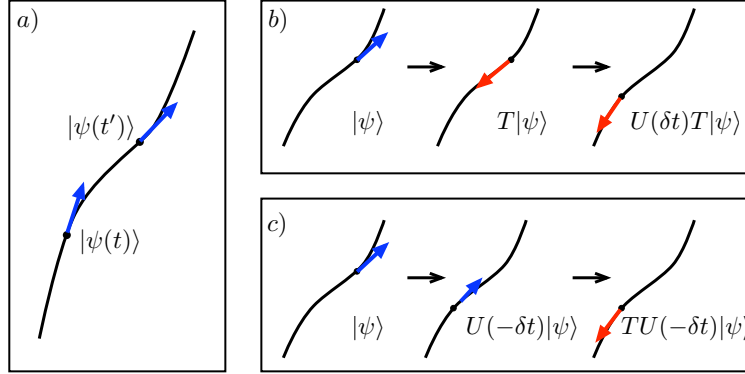
Figure 1.4. Time evolution represented as a flow along a "worldline" in Hilbert space (a). In time reversal symmetric systems, reversing the motion and evolving forward in time (b) is equivalent to evolving backwards in time and then reversing the motion (c). The b (c) panel pictorially represents the left (right) hand side of Eq. (1.51).

"direction" of motion[22]. Applying the time reversal operator T at a given time t_0, reverses the motion of the ket. Therefore if we have time reversal symmetry

$$U(t_0, t_0 + \delta t)T \left| \psi(t_0) \right\rangle = TU(t_0, t_0 - \delta t) \left| \psi(t_0) \right\rangle. \qquad (1.51)$$

This equation reads in words: first reversing the motion and then evolving *forwards* in time, is equivalent to first evolving *backwards* in time and then reversing the motion (cf. Fig. 1.4).

For δt infinitesimal, $U(t_0, t_0 \pm \delta t) = 1 \mp iH\delta t/\hbar$, and since the time reversal relation (1.51) has to be valid for all kets $\left| \psi(t_0) \right\rangle$

$$(1 - iH\delta t/\hbar)T = T(1 + iH\delta t/\hbar). \qquad (1.52)$$

If T were linear this would mean that $HT = -TH$, and thus for any energy eigenvalue E there would be an accompanying energy eigenvalue

---

[22]The arrows represent the Hamiltonian flow in Hilbert space, the Hamiltonian being the generator of time translation. It is perfectly fine, for intuition, to imagine the arrows being the direction of momentum.

$-E$. This is clearly a nonsensical result (take for example free electrons which have a strictly positive spectrum). Therefore we need to take T to be antilinear (and antiunitary) and find

$$[H, T] = 0. \tag{1.53}$$

In contrast to a unitary operator that commutes with the Hamiltonian, relation (1.53) does not lead to a conserved quantity. The reason is that because T is antilinear $TU(t, t') \neq U(t, t')T$ even though (1.53) is satisfied. Thus, an eigenstate of T does not necessarily remain an eigenstate of T under time evolution (contrast this with linear and unitary symmetries).

Spinless Systems

In a spinless system, the unitary operator U in $T = U\mathcal{C}$ for the conventional time reversal is simply equal to unity if $\mathcal{C}$ is taken to be with respect to the position basis $\{|x\rangle\}$. To see this consider the action of $\mathcal{C}\hat{x}$ on a general state vector $|\psi\rangle$

$$\mathcal{C}\hat{x}\,|\psi\rangle = \mathcal{C}\int dx\,x\,\psi(x)\,|x\rangle = \int dx\,x\,\psi^*(x)\,|x\rangle = \hat{x}\,\mathcal{C}\,|\psi\rangle. \tag{1.54}$$

Similarly for the momentum operator $\hat{p}$ we find

$$\mathcal{C}\hat{p}\,|\psi\rangle = \mathcal{C}\int dx\,(-i\hbar\partial_x\psi)\,|x\rangle = -\int dx\,(-i\hbar\partial_x\psi^*)\,|x\rangle = -\hat{p}\,\mathcal{C}\,|\psi\rangle. \tag{1.55}$$

These relations are valid for all $|\psi\rangle$ so the operators have to satisfy

$$\mathcal{C}\hat{x}\,\mathcal{C}^{-1} = \hat{x}, \tag{1.56a}$$

$$\mathcal{C}\hat{p}\,\mathcal{C}^{-1} = -\hat{p}. \tag{1.56b}$$

This is indeed what we want from our time reversal operator, and thus $T = \mathcal{C}$. Note that since $\mathcal{C}^2 = 1$ the time reversal operator squares to one in the spinless case.

Spin $\frac{1}{2}$ System

With the position operator even under time reversal and the momentum operator odd, the orbital angular momentum $\boldsymbol{L} = \boldsymbol{x} \times \boldsymbol{p}$ is clearly odd. Any angular momentum, in particular the spin, should therefore also be odd[23]. Extending the complex conjugation to be with respect to the tensor product $|x\rangle \otimes |\pm\rangle$ of position basis and the eigenstates $|\pm\rangle$ of σ_3, it becomes clear that $\mathcal{C}$ is not sufficient to represent time reversal. We need to find a unitary operator U such that $T\boldsymbol{\sigma}T^{-1} = U\boldsymbol{\sigma}^*U^\dagger = -\boldsymbol{\sigma}$. In components

$$U\sigma_1 U^\dagger = -\sigma_1, \tag{1.57}$$

$$U\sigma_2 U^\dagger = \sigma_2, \tag{1.58}$$

$$U\sigma_3 U^\dagger = -\sigma_3. \tag{1.59}$$

σ_2 does the job, but we are free to choose an accompanying phase. In anticipation of later discussion we will choose the phase such that

$$T = -i\sigma_2 \mathcal{C}. \tag{1.60}$$

In this case $T^2 = -1$ while in the spinless case $T^2 = 1$. This generalizes: Systems with integral spin (even number of spin half particles) have a time reversal that squares to 1, while for half integral spin systems (odd number of spin half particles) it squares to -1 [13].

1.2.4   Consequences of Time Reversal for Hamiltonians

From now on we will exclusively consider the consequences of time reversal in spin half systems, or more generally in system were $T^2 = -1$.

Assume that $|E_n\rangle$ is an eigenstate of H with eigenvalue E_n and that H is time reversal symmetric. H and T then commute [cf. Eq. (1.53)], and $T|E_n\rangle$ is also an eigenstate with eigenvalue E_n. Furthermore, using the relation (1.39) and $T^2 = -1$, these two states are seen to be orthogonal

$$\langle E_n | T E_n \rangle = \langle T E_n | T^2 E_n \rangle^* = -\langle E_n | T E_n \rangle \tag{1.61}$$

---

[23]This argument can be made more rigorous by considering the transformation of the total angular momentum $J = L + S$ [14].

i.e. $\langle E_n|TE_n\rangle = 0$. Every eigenvalue of the Hamiltonian is thus necessarily twofold degenerate. This is the Kramers degeneracy (of energy eigenvalues) [11, 12].

The arguments used in (1.61) did not rely on $|E_n\rangle$ being an eigenstate of H, and it thus true that any state $|n\rangle$ is orthogonal to its time reverse $T|n\rangle = |Tn\rangle$. We can thus generally[24] adopt an orthogonal basis set $\{|n\rangle, |Tn\rangle\}$ [15]. What is the form of the time reversal operator in this basis? A general state $|\psi\rangle$ can be written

$$|\psi\rangle = \sum_m (\psi_{m,+}|m\rangle + \psi_{m,-}|Tm\rangle). \tag{1.62}$$

Acting on this state with T (using antilinearity and $T^2 = -1$)

$$T|\psi\rangle = \sum_m (\psi_{m,+}^*|Tm\rangle - \psi_{m,-}^*|m\rangle). \tag{1.63}$$

We notice that T does not couple states with different m. We can thus look at a 2×2 submatrix (quaternion) of T, spanned by the states $|m\rangle$ and $|Tm\rangle$. As usual, writing $T = U\mathcal{C}$ the complex conjugation operator takes care of the complex conjugation. Inspection of Eq. (1.63) then leads us to take

$$U_{nm} = \begin{pmatrix} \langle n|U|m\rangle & \langle n|U|Tm\rangle \\ \langle Tn|U|m\rangle & \langle Tn|U|Tm\rangle \end{pmatrix} = \delta_{nm} \begin{pmatrix} 0 & -1 \\ 1 & 0 \end{pmatrix} = -i\sigma_2 \delta_{nm}. \tag{1.64}$$
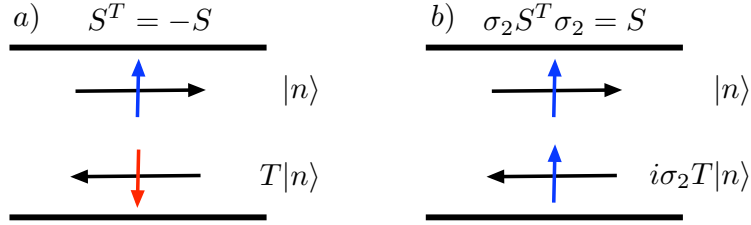
In the quaternionic notation $U = -i\sigma_2$ (tensor product with the unit matrix is implied) and $T = -i\sigma_2\mathcal{C}$. This agrees with the result (1.60) for the conventional time reversal but is more general.

Writing H in the same basis, time reversal invariance requires the Hamiltonian to be quaternionic real

$$H = THT^{-1} = -i\sigma_2\mathcal{C}H\mathcal{C}i\sigma_2 = \sigma_2 H^*\sigma_2 = \tilde{H}. \tag{1.65}$$

---

[24]It is relatively straightforward to see that this can always be done. Start with $|1\rangle$ and $|T1\rangle$. Choose $|2\rangle$ orthogonal to $|1\rangle$ and $|T1\rangle$ (for example using the Gram-Schmidt process). Then antiunitary of T guarantees that $|T2\rangle$ is orthogonal to all the other basis vectors chosen. Continue this process until you have a full basis.

$a)$ $S^T = -S$ $b)$ $\sigma_2 S^T \sigma_2 = S$

                              $|n\rangle$ $|n\rangle$

                              $T|n\rangle$ $i\sigma_2 T|n\rangle$

Figure 1.5. A schematic picture of the scattering states used as a basis for the scattering matrix. On the left the outgoing state is the time reverse of the incoming state, while on the left the spin is flipped such that the spin state of the incoming and outgoing states is the same.

Since H is hermitian, this implies that the Hamiltonian is also self-dual $H^R = H$.

1.2.5   Consequences of Time Reversal for Scattering Matrices

The presence of time reversal has implications also for the symmetry of the scattering matrix. The exact way this symmetry is reflected in the scattering matrix depends on the basis chosen. We will here discuss a couple of cases.

Symmetry of S

We consider a conventional two terminal scattering setup with $N_{L(R)}$ modes in the left (right) lead. We will label all incoming states on the left (right) with $|n\rangle$ ($|m\rangle$). The outgoing modes will then be $|Tn\rangle$ ($|Tm\rangle$). A general scattering state $|\varphi\rangle$ will then have the following form in the left lead

$$|\varphi\rangle = \sum_{n=1}^{N_L} (c_n^{\text{in,L}} |n\rangle + c_n^{\text{out,L}} |Tn\rangle), \tag{1.66}$$

and similar for the right lead (with $L \to R$ and $n \to m$). The scattering matrix connects the vectors of coefficients c^{in} to c^{out}

$$\begin{pmatrix} c^{\text{out,L}} \\ c^{\text{out,R}} \end{pmatrix} = S \begin{pmatrix} c^{\text{in,L}} \\ c^{\text{in,R}} \end{pmatrix} = \begin{pmatrix} r & t' \\ t & r' \end{pmatrix} \begin{pmatrix} c^{\text{in,L}} \\ c^{\text{in,R}} \end{pmatrix} \tag{1.67}$$

If we have time reversal symmetry then

$$T \left| \varphi \right\rangle = \sum_{n=1}^{N_L} [(c_n^{\text{in,L}})^* \left| Tn \right\rangle - (c_n^{\text{out,L}})^* \left| n \right\rangle), \tag{1.68}$$

is also a scattering state with the same energy. That means that

$$\begin{pmatrix} (c^{\text{in,L}})^* \\ (c^{\text{in,R}})^* \end{pmatrix} = S \begin{pmatrix} -(c^{\text{out,L}})^* \\ -(c^{\text{out,R}})^* \end{pmatrix}. \tag{1.69}$$

Multiplying from the left with $S^\dagger$, using unitarity of S and complex conjugating

$$\begin{pmatrix} c^{\text{out,L}} \\ c^{\text{out,R}} \end{pmatrix} = -S^T \begin{pmatrix} c^{\text{in,L}} \\ c^{\text{in,R}} \end{pmatrix}. \tag{1.70}$$

We conclude, by comparison with Eq. (1.67), that S is antisymmetric[25]

$$S = -S^T. \tag{1.71}$$

Note that this means that the diagonal elements are zero in agreement with the qualitative discussion of weak antilocalization in Sec. 1.1.3.

The representation (1.71) is most natural from the point of view of time reversal, and it is completely general. It is however rarely, if ever, seen in the literature. To understand why, consider the diagonal elements of the reflection matrix r (see Fig. 1.5). In our representation these elements

---

[25]In a typical calculation $|n\rangle$ could for example be a plane wave times a spinor. Often one would then want to use the same basis state to be an incoming state on the left and an outgoing state on the right. Thus the scattering state on the left would have the form (1.66) on the left, but on the right $|n\rangle$ and $|Tn\rangle$ would change role. With similar calculation as above, one finds that in this case $S = -\tau_z S^T \tau_z$, with $\tau_z = \begin{pmatrix} 1 & 0 \\ 0 & -1 \end{pmatrix}$ in the block structure of the scattering matrix.

describe processes where a spin up[26] particle is reflected as a spin down particle. In some cases there is only one band (like single-valley graphene) and the direction of the spin is completely tied to the momentum direction, and this is then the only meaningful representation. Quite often though, we have two degenerate bands (leads without spin-orbit coupling), and the most common representation is where a spin up particle is reflected as a spin up particle. We can easily take this into account in our scattering state, simply by flipping the spin of the outgoing mode (using $i\sigma_2$), which then becomes

$$|\varphi\rangle = \sum_{n=1}^{N_L} \sum_{\sigma=\pm} (c_{n,\sigma}^{\text{in,L}} |n,\sigma\rangle + c_{n,\sigma}^{\text{out,L}} i\sigma_2 T |n,\sigma\rangle), \qquad (1.72)$$

with $|n,\sigma\rangle = |n\rangle \otimes |\sigma\rangle$ and σ_2 acts on $|\sigma\rangle$. Going through the same calculation that lead to Eq. (1.71), we obtain the well known result that the scattering matrix is self-dual

$$S = \sigma_2 S^T \sigma_2 = S^R. \qquad (1.73)$$

Note that this representation is only possible when we have an even number of modes.

Kramers Degeneracy of Transmission Eigenvalues

The Kramers degeneracy of energy eigenvalues in time reversal symmetric systems is intuitively understandable: An electron moving to the left surely has the same energy as a particle moving to the right. The Kramers degeneracy of transmission eigenvalues (eigenvalues of the product $tt^\dagger$ of the matrix t of transmission amplitudes) is much less intuitively clear. In fact, time reversal takes an incoming mode into an outgoing mode, so why should there be any degeneracy. This lack of an intuitive picture plus the absence of a simple proof[27] for this fact has lead to a certain lack

---

[26]The quantization axis with respect to which *up* is defined depends on the problem at hand and can even depend on the quantum number n.

[27]To quote the authors of Ref. 19: "Note that the proof of the Kramers degeneracy of transmission eigenvalues is by far more complicated than that of the original Kramers theorem for the degeneracy of energy levels".

of appreciation for it, despite it being widely known. In this section we present a new alternative proof for this Kramers degeneracy, given solely in terms of the symmetries of the scattering matrix.

We have seen that in the presence of time reversal the scattering matrix is antisymmetric. In particular the reflection matrix r is antisymmetric $r^T = -r$. A linear algebra theorem [20, 21] states that for any antisymmetric matrix r there exist a unitary matrix W such that $r = W^T D W$, with

$$D = \Sigma_1 \oplus \Sigma_2 \oplus \cdots \oplus \Sigma_k \oplus 0 \oplus \cdots \oplus 0, \qquad (1.74)$$

where $2k = \text{rank } r$, $\oplus$ denotes the direct sum and

$$\Sigma_j = \begin{pmatrix} 0 & \lambda_j \\ -\lambda_j & 0 \end{pmatrix}, \quad \lambda_j > 0, \quad j = 1, \cdots, k. \qquad (1.75)$$

In other words, D is block diagonal with k 2×2 nonzero blocks Σ_j and $N_L - 2k$ 1×1 zero blocks 0. Clearly if there are odd number of modes (i.e. the dimension of r is odd) there is at least one zero term in the sum (1.74). Using this result, we find that

$$r^\dagger r = W^\dagger D^T D W. \qquad (1.76)$$

But since

$$\Sigma_r^T \Sigma_r = \begin{pmatrix} \lambda_r^2 & 0 \\ 0 & \lambda_r^2 \end{pmatrix}, \qquad (1.77)$$

we have managed to diagonalize $r^\dagger r$ and found that its eigenvalues come in pairs. Due to unitarity of S, $\mathbb{1} - r^\dagger r$ and $t^\dagger t$ have the same eigenvalues. The transmission eigenvalues are thus twofold degenerate (Kramers degeneracy), plus (if the number of modes is odd) one eigenvalue equal to unity (perfect transmission [22]).

1.3   Model Hamiltonians

In order to demonstrate the theory we have been discussing, we will in this section find the eigenstates and eigenenergies of two model Hamiltonians: The Rashba Hamiltonian of Sec. 1.1.4 and the single valley graphene Dirac
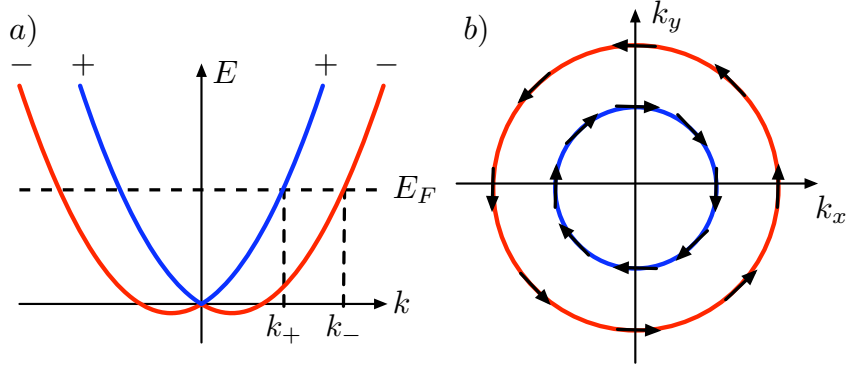
Figure 1.6. (a) The energy band structure of the Rashba Hamiltonian with the definition of the momenta $k_\pm$. (b) The Fermi surface consists of two concentric circles of radius $k_\pm$. The black arrows show the spin direction of the energy eigenstates.

Hamiltonian. In the latter the spin degree of freedom is not the real spin but rather the pseudospin corresponding to a sublattice index of the envelope wavefunction [23–25]. Similarly the time reversal is not the real time reversal but rather another antiunitary symmetry sometimes called effective time reversal.

1.3.1 The Rashba Hamiltonian

As a prototypical example of a simple electronic system with spin-orbit coupling, we consider in this section the Rashba Hamiltonian

$$H_R = \frac{p^2}{2m} + \frac{\alpha}{\hbar}(p_y \sigma_1 - p_x \sigma_2). \tag{1.78}$$

Since H_R commutes with the momentum operator $\boldsymbol{p}$ the eigenstates can be taken to be of the form $|\psi\rangle = |\boldsymbol{k}\rangle \otimes |\chi\rangle$ with $\langle \boldsymbol{x}|\boldsymbol{k}\rangle = \exp(i\boldsymbol{k} \cdot \boldsymbol{x})$. $|\chi\rangle$ is found by diagonalizing H_R for a fixed $\boldsymbol{k} = k(\cos\phi\,\hat{x} + \sin\phi\,\hat{x})$

$$H_R = \frac{\hbar^2 k^2}{2m} \begin{pmatrix} 1 & i\tilde{\alpha}e^{-i\phi} \\ -i\tilde{\alpha}e^{i\phi} & 1 \end{pmatrix}, \tag{1.79}$$

where $\tilde{\alpha} = 2m\alpha/(\hbar^2 k)$. The eigenvalues

$$\varepsilon_\pm = \frac{\hbar k^2}{2m} \pm \alpha k, \tag{1.80}$$

are independent of ϕ and show a zero (magnetic) field spin-splitting (see Fig. 1.6). The eigenstates $|\chi\rangle$ are found to be

$$|\chi_\pm(\phi)\rangle = \frac{1}{\sqrt{2}} \begin{pmatrix} e^{-i\phi/2} \\ \mp i e^{i\phi/2} \end{pmatrix}. \tag{1.81}$$

From these states we find that the direction of the spin,

$$\hat{n}_\pm = \langle \chi_\pm | \boldsymbol{\sigma} | \chi_\pm \rangle = (\pm \sin\phi, \mp \cos\phi, 0), \tag{1.82}$$

is orthogonal to the momentum $\hat{\mathbf{k}} \cdot \hat{n}_\pm = 0$. This can be summarized in the equation

$$\hat{n}_\pm = \pm \hat{\boldsymbol{k}} \times \hat{z}, \tag{1.83}$$

with $\hat{z}$ the unit vector in the z direction. We will sometimes refer to a spin with $\hat{n}_+$ ($\hat{n}_-$) as a plus (minus) spin. For a given energy the Fermi surface consists of two concentric circles with radii (Fig. 1.6)

$$k_\pm = \sqrt{k_{\mathrm{so}}^2 + k_F^2} \mp k_{\mathrm{so}}, \tag{1.84}$$

with $k_{\mathrm{so}} = \alpha m/\hbar$ and $k_F = \sqrt{2mE_F}/\hbar$ the Fermi wavevector. The spin rotates as we go along the circles such that there is no zero field spin polarization, consistent with time reversal symmetry.

A neat way of picturing this is to write the Rashba spin-orbit term as Zeeman splitting with a momentum dependent magnetic field

$$H_R = -\boldsymbol{B}(\boldsymbol{p}) \cdot \boldsymbol{\sigma}; \quad \boldsymbol{B}(p) = \alpha(-p_y, p_x, 0) = -\hbar\alpha\, \boldsymbol{k} \times \hat{z}. \tag{1.85}$$

The spin eigenstate $\left| \chi_{-(+)} \right\rangle$ is (anti)parallel to the field.

It is instructive to see explicitly that transforming a state with the time reversal operator $T = -i\sigma_2 \mathcal{C}$ gives us another eigenstate. In fact

$$T \left| \chi_\pm(\phi) \right\rangle = \pm \left| \chi_\pm(\phi + \pi) \right\rangle, \tag{1.86}$$

i.e. time reversal connects states on the same Fermi surface circle.

We gained some insight into the role of time reversal by looking at the eigenstates of the Hamiltonian. Being diagonal in that basis, the Hamiltonian is trivially quaternionic real. Let us get a bit more acquainted with the abstract theory of the last section by calculating the Hamiltonian in the states $|\phi, \pm\rangle$ where

$$\langle \boldsymbol{x}|\phi, +\rangle = \exp(i\boldsymbol{k}\cdot\boldsymbol{x}) \begin{pmatrix} \xi_\phi \\ 0 \end{pmatrix}, \tag{1.87a}$$

$$\langle \boldsymbol{x}|\phi, -\rangle = \exp(i\boldsymbol{k}\cdot\boldsymbol{x}) \begin{pmatrix} 0 \\ 1 \end{pmatrix}. \tag{1.87b}$$

The phase factor

$$\xi_\phi = \begin{cases} +1 & 0 \le \phi < \pi \\ -1 & \pi \le \phi < 2\pi \end{cases} \tag{1.88}$$

ensures that

$$T\,|\phi, \pm\rangle = |\phi + \pi, \mp\rangle. \tag{1.89}$$

A quaternion of the Hamiltonian in this basis ordered like in (1.64) (with $|n\rangle = |\phi, \pm\rangle$) thus becomes[28]

$$H_{\phi+,\phi'-} = \begin{pmatrix} \langle \phi, +|H|\phi', -\rangle & \langle \phi, +|H|\phi'+\pi, +\rangle \\ \langle \phi+\pi, -|H|\phi', -\rangle & \langle \phi+\pi, -|H|\phi'+\pi, +\rangle \end{pmatrix}$$
$$= \alpha k\,(\sin\phi\,\mathbb{1} + \cos\phi\,i\sigma_3)\delta_{\phi,\phi'}. \tag{1.90}$$

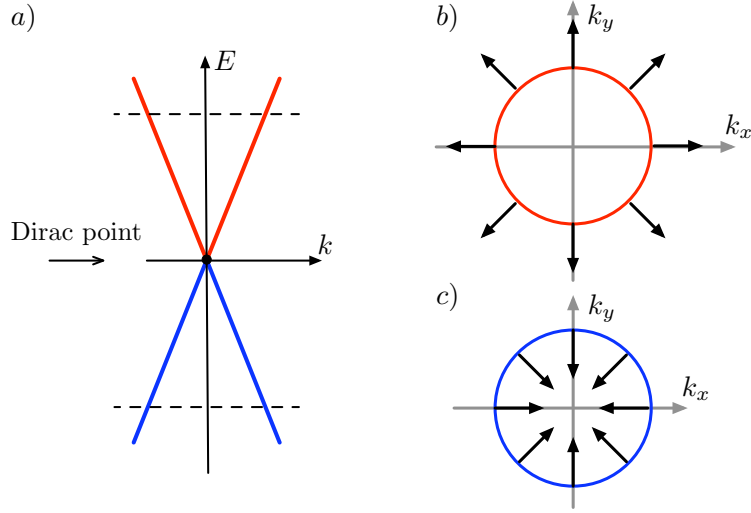The rest of the Hamiltonian quaternions are obtained similarly,

$$H_{\phi\pm,\phi'\pm} = \frac{\hbar^2 k^2}{2m}\delta_{\phi,\phi'}\mathbb{1}, \tag{1.91a}$$

$$H_{\phi-,\phi'+} = \alpha k\,(\sin\phi\,\mathbb{1} - \cos\phi\,i\sigma_3)\delta_{\phi,\phi'} = H^R_{\phi+,\phi'-}. \tag{1.91b}$$

The Hamiltonian is indeed quaternionic real and self-dual as expected.

---

[28]To avoid double counting in the basis $(\{|\phi, \pm\rangle, T\,|\phi, \pm\rangle\})$ we restrict $0 \le \phi, \phi' < \pi$.

Figure 1.7.   (a) The conical energy dispersion relation of a single valley graphene, with the two cones touching at the Dirac point. (b) In the conduction (valence) band the direction of the pseudospin is (anti)parallel to the momentum.

1.3.2   Graphene - the Single Valley Dirac Hamiltonian

In graphene, in the absence of intervalley scattering, the low energy excitations are described by the Dirac Hamiltonian

$$H = v\boldsymbol{p} \cdot \boldsymbol{\sigma} \qquad (1.92)$$

with $v \approx c/300$ the velocity of the massless excitations. The energy eigenstates are $\langle \boldsymbol{x}|\varphi, \pm \rangle = \exp(i\boldsymbol{k} \cdot \boldsymbol{x}) |\chi_{\pm}(\varphi)\rangle$ with $\boldsymbol{k} = k(\cos\varphi \, \hat{x} + \sin\varphi \, \hat{y})$ and

$$|\chi_{\pm}(\varphi)\rangle = \frac{e^{\mp i\pi/4}}{\sqrt{2}} \begin{pmatrix} \pm e^{-i\varphi/2} \\ e^{i\varphi/2} \end{pmatrix}. \qquad (1.93)$$

With the phase factor $e^{\mp i\pi/4}$ these states satisfy $T |\varphi, \pm \rangle = |\varphi + \pi, \pm \rangle$, with $T = -i\sigma_2 \mathcal{C}$. The spectrum

$$\varepsilon_{\pm} = \pm v\hbar k, \qquad (1.94)$$

consists of two cones whose apexes meet in a single point called the Dirac point (see Fig. 1.7). The direction of the pseudospin

$$\hat{n}_\pm = \langle \chi_\pm | \boldsymbol{\sigma} | \chi_\pm \rangle = \pm(\cos\varphi, \sin\varphi, 0) = \pm\hat{k} \qquad (1.95)$$

is always parallel to the group velocity $\boldsymbol{v}_{g\pm} = \pm v\hat{k}$. Calculating the matrix elements of the Hamiltonian in the basis (1.87) of eigenstates of σ_z in analogous way to the last section, one finds that the Hamiltonian matrix is quaternionic real and self-dual.

1.4   This Thesis

We end this introduction with a brief introduction to the remaining chapters.

Chapter 2: Stroboscopic Model of Transport Through a Quantum Dot with Spin-Orbit Coupling

In the physicist's toolbox, simple models that capture the essential physics and allow for an analytical solution are the best. These are rare. In their absence simple models that capture the essential physics and allow for an efficient numerical simulation are invaluable, be it for the sole purpose of comparing to (often approximate) analytical calculations, or even simulating experiments that can not be conducted in the lab with current technology. A numerical experiment, if you like.

The spin kicked rotator is just such a model; It generalizes the open spinless kicked rotator, which is used to model quantum transport through ballistic quantum dots, to include spin and spin-orbit coupling. The open kicked rotator, in turn, is a generalization of the kicked rotator, which models closed chaotic quantum dots, to model transport. The kicked rotator is a model of a pendulum (or a rotator) that rotates around a fixed point (in the absence of gravity) and is kicked periodically with an essentially random kicking strength. The time dependence is needed, for without it energy would be a constant of the motion and the model would be integrable.

In chapter 2 we introduce the open spin (symplectic) kicked rotator in the traditional way. That is, quantize the Hamiltonian and reduce its one period time evolution operator, the Floquet operator $\mathcal{F}$, to a discrete finite form by going to parameter values that give what is called a resonance. To be consistent with prior literature it is important to do it this way. For physical intuition, however, it is more fruitful to consider the Floquet operator

$$\mathcal{F} = \Pi U X U^{\dagger} \Pi \qquad (1.96)$$

as the definition of the model. One then considers the matrix X to describe the free (spin-orbit coupled) motion inside the chaotic cavity. This free motion is interrupted by boundary scattering which is given in terms of the matrix Π. (The matrix X is diagonal in θ space, while Π is diagonal in p-space; U maps between the two spaces. θ and p are conjugate variables.) With this interpretation, the variable θ becomes the momentum-like variable, while p becomes a variable for the position on the boundary. To accommodate the notation it can be useful to think of θ as the angle describing the direction of the momentum.

How one then goes on to open up the model, i.e. attach leads, is described in the chapter. There it is explained how one needs to consider an alternative time reversal symmetry to the one usually used for the spinless kicked rotator. With the above interpretation in mind, the reasons for this are physically clear.

By simply looking at the model, it is by no means clear how to relate its parameters (kicking strengths and symmetry breaking parameters) to a real physical system. With some simple assumptions, we calculate analytically the conductance of the spin kicked rotator, and by varying parameters we can go from weak localization to weak antilocalization, to the absence of weak localization (which happens in the presence of magnetic field). By direct comparison with results from random-matrix theory, one reads off the connection between the model parameters and the physical parameters (magnetic field, spin-orbit coupling time etc.). This is a valuable result for any estimate of physical scales in the model.
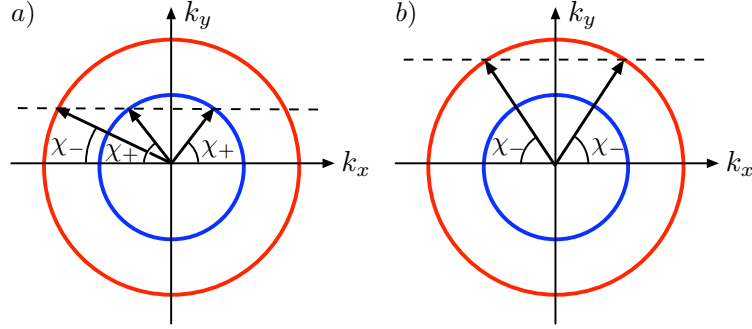
Figure 1.8. A $+$ spin plane wave incident on a hard wall with an incident angle χ_+ (a) is always reflected as two plane waves with reflection angles $\chi_\pm$. A $-$ spin plane wave (b) can, on the other hand, for large enough incident angles be reflected as a single plane wave .

Chapter 3: How Spin-Orbit Coupling Can Cause Electronic Shot Noise

In the absence of spin-orbit coupling, a plane wave incident on a hard wall is reflected as a single plane wave with an angle of reflection equal to the angle of incidence. In the presence of spin-orbit coupling this is no longer true; the plane wave can be reflected as two plane waves.

This can be understood pictorially as shown in Fig. 1.8, were we consider the case that the Fermi surface consists of two concentric circles (as in the Rashba case in Sec. 1.3.1). Assuming that the hard wall is parallel to the y-axis, the y component k_y of the momentum is conserved. If the incoming way belongs to the inner circle ($+$ spin plane wave) there are two possibilities for the outgoing wave. An incoming wave on the outer circle ($-$ spin) also has two possible outgoing waves, unless the angle of incident χ_- is larger then the critical angle $\chi_c = \arcsin(k_+/k_-)$ with $k_+(k_-)$ the radius of the inner (outer) Fermi circle [cf. Eq. (1.84)]. When there are two outgoing waves, we talk of trajectory splitting [26].

Can this trajectory splitting be a source of (shot) noise in a ballistic quantum dot? That is the question considered in chapter 3. The answer is yes, but to observe it one needs to suppress any other sources of shot noise, in particular the shot noise that arises by the simple fact that the

electron is a wave. Imagine an electron trying to impinge on a lead. If the electron wavepacket is spread over a length scale large then the lead opening, it is going to be partially reflected, causing shot noise. To get rid of this source of noise one needs simply to make the lead very large, such that the spread of the wavepacket is negligible. In this chapter, this condition is given in terms of the Ehrenfest time τ_E, which essentially is the time it takes a wavepacket to spread to the size of the leads. If the dwell time τ_{dwell}, the time the electron spends inside the quantum dot, is smaller then the Ehrenfest time, quantum mechanical wave noise does not play any role.

We establish that in this limit there is a parameter regime were the trajectory splitting is the dominant source of shot noise. To check our theory, we have compared to a numerical simulation of classical particles in a stadium billiard. The trajectory splitting is calculated quantum mechanically, and added to the classical equations of motions to determine what happens as the classical particles are reflected of the boundaries of the billiard. The numerical results are found to be in agreement with our theory.

Chapter 4: Degradation of Electron-Hole Entanglement by Spin-Orbit Coupling

Take a tunnel junction connecting two metals and apply a voltage across it. Every now and then, and electron will tunnel from one side, leaving a hole behind on the other. The electron-hole pair move in opposite directions, creating a current that you can measure; the tunneling current. There is more to this simple process. Namely, the electron and the hole turn out to be entangled [27].

In chapter 4 we consider how the presence of spin-orbit coupling affects this electron-hole entanglement. In order to do so we begin by generalizing an earlier result to include many modes. The reason for this is that the degradation of the entanglement arises because of mode mixing by the spin-orbit coupling.

To quantify the entanglement we use the concurrence. The concurrence depends essentially on two parameters: the number of modes N in the leads connecting the tunnel barrier to the reservoirs, and the ratio $\tau_{\mathrm{dwell}}/\tau_{\mathrm{so}}$ of
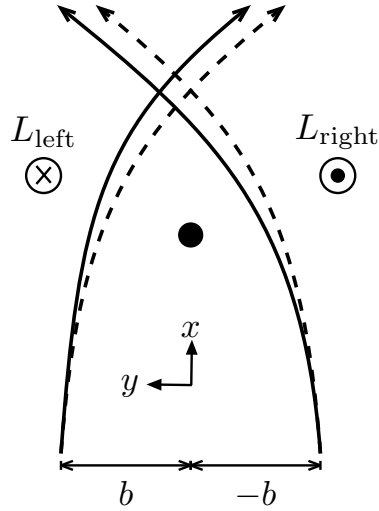
Figure 1.9. A schematic of a scattering of spin up (with respect to z axis) particles by a massive spinless particle (black dot in center). Dashed lines show the symmetric trajectories of electrons with impact parameters b and $-b$, realized when the spin-orbit coupling is neglected. Spin-orbit coupling makes the potential of the scatterer more (less) attractive for particles passing on the right (left), causing a left-right asymmetry in the scattering (solid trajectories).

the time the electron-hole pairs spends in the leads τ_{dwell} and the spin-orbit coupling time τ_{so}. The dependence of the concurrence on both these parameters can be understood intuitively. The more modes there are, the bigger the possibility of mode mixing and the smaller the concurrence. The longer time the modes have to mix, the smaller the concurrence, with τ_{so} setting the time scale on which it goes to zero.

We confirm these expectations numerically, and find in addition that for large number of modes the concurrence is independent of the number of modes. This allows us to make a simplifying assumption (about the form of the spin density matrix) in order to analytically calculate the dependence of the concurrence on the ratio $\tau_{\mathrm{dwell}}/\tau_{\mathrm{so}}$. We find good agreement between our analytical calculation and our numerics.

Chapter 5: Mesoscopic Spin Hall Effect

Let us consider scattering of a spin-half particle by a massive spinless particle [28]. According to our discussion in Sec. 1.1.1 [in particular Eq. (1.7)] the scattering potential the spin-half particle sees will be of the form

$$V_{\text{sc}} = V_0 + V_s(r)\boldsymbol{\sigma} \cdot \boldsymbol{L}. \tag{1.97}$$

Imagine sending in a beam of spin up (with respect to the z-axis) particles with a random impact parameter b. Neglecting the spin-orbit coupling, electrons with impact parameter b and $-b$ will scatter symmetrically (dashed lines in Fig. 1.9). When taking into account the spin-orbit coupling, the electrons passing on the right (left) of the scatterer have an angular momentum parallel (antiparallel) to the spin, and thus feel a stronger (weaker) potential. When averaging over all b we find that spin up electrons have a net tendency to scatter to the left [28]. Spin down electrons on the other hand have a net tendency to scatter to the right. An unpolarized incident beam in the x direction will thus, due to spin-orbit coupling, generate a pure spin current (i.e. not accompanied by a charge current) flowing in the y direction (polarized in the z direction). This, in essence, is the spin Hall effect [29, 30].

The above mechanism is *extrinsic*, coming e.g. from impurities. The *intrinsic* mechanisms for spin-orbit coupling, like the Rashba term, also give arise to a spin Hall effect. To understand this, we recall the representation (1.85) of the Rashba term as a momentum dependent magnetic field. In equilibrium the spin eigenstates are (anti)parallel to this magnetic field, but applying an electric field E_x accelerates the electrons, changing the momentum and in turn the Rashba magnetic field the spin sees. This leads to a precession of the spin out of plane, leading to a spin current $j_{s,y}$ (in the z direction) in analogy to the case discussed above. Referring to Fig. 1.6, the two states at each momentum give a contribution that cancel out. It is thus only the states in the annulus $k_+ < k < k_-$ that contribute, giving a spin Hall conductance [31]

$$\sigma_{sH} = -\frac{j_{s,y}}{E_x} = \frac{e}{8\pi}. \tag{1.98}$$

In the presence of disorder, however, this spin Hall conductance averages to zero [32]. Essentially, the diffusive scattering scrambles the momentum and the Rashba field such that the precession of the spin averages to zero.

In chapter 5 we consider the spin Hall effect in a mesoscopic four terminal chaotic cavity with spin-orbit coupling. The voltages on the terminals are adjusted such that a charge current flows between two longitudinal leads, while no charge current flows in the two transverse leads. In analogy to the two cases discussed above, the spin-orbit coupling gives arise to spin currents in the transverse leads, but the chaotic dynamics (like diffusion) scrambles the momentum such that on average this spin current is zero.

Even though the average spin current is zero, the variance does not need to be. In fact, one expects different cavities to contribute differently to the mean. By changing the chaotic dynamics (e.g. by changing the shape of the cavity) one thus expects spin current fluctuations, very much in analogy to conductance fluctuations. In this chapter we calculate this spin current fluctuations using random-matrix theory, and show that it is universal (in the same sense as universal conductance fluctuations are universal). In order to check our analytical predictions we compare with numerical simulations using the spin kicked rotator of chapter 2.

Chapter 6: One-Parameter Scaling at the Dirac Point in Graphene

Suppose you have a chunk of disordered material of volume L^d with d its dimension. Imagine doubling all the lengths such that the volume becomes $(2L)^d$, made up of 2^d pieces of the original size. Is there a relationship between the conductance of the larger chunk and the conductance of its constituent smaller chunks? According to the scaling theory of localization [33, 34] there is and in fact the rate of change of the dimensionless conductance $g = G/(e^2/h)$ can be written in terms of the beta function

$$\beta(g) = \frac{d \ln g}{d \ln L} \tag{1.99}$$

which depends only on the single parameter g.

In the Drude theory of metals the conductivity σ is a constant and the conductance $G = \sigma L^{d-2}$. For large conductance ($g \gg 1$) we expect the
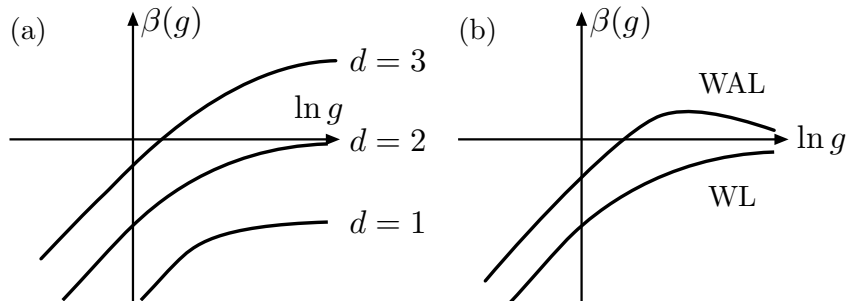
Figure 1.10. (a) A schematic of the beta function of the scaling theory of localization in different dimensions. (b) In two dimension how the beta function approaches zero becomes critical. This is determined by the weak (anti)localization (WL/WAL) correction to the conductivity. In the presence of spin-orbit coupling the beta function approaches zero from above.

Drude theory to be accurate, and thus in this limit

$$\lim_{g \to \infty} \beta(g) = d - 2. \tag{1.100}$$

On the other hand, if the disorder is large enough, the electron wavefunction localizes and the conductance is exponentially small $g \propto \exp(-L/\xi)$ with ξ the localization length. Thus

$$\lim_{g \to 0} \beta(g) = \ln g. \tag{1.101}$$

Assuming that these two limits are connected in a continuous and monotonous manner [33], we obtain the beta functions sketched in Fig. 1.10.

In the two dimensional case, the beta function goes to zero in the limit of large conductance. It therefore is important to know how this limit is approached. This one can do by a perturbation theory around the perfect metal assuming weak disorder. The result is the phenomena of weak (anti) localization discussed in Sec. 1.1.3, but in disordered systems it takes the form [35]

$$\sigma = \sigma_0 - \frac{2 - \beta}{\beta} \frac{e^2}{h} \frac{2}{\pi} \ln L/\ell, \tag{1.102}$$

with ℓ the mean free path, and $\beta = 1(4)$ in the absence (presence) of spin-orbit coupling (see also Sec. 2.3). We thus observe that in the presence (absence) of spin-orbit coupling the beta function approaches zero from above (below) as $\beta(g) \sim +1/\pi g$ ($\beta(g) \sim -2/\pi g$).

In graphene, intervalley scattering leads to localization [36, 37]. This means that for system sizes L much larger then the intervalley scattering length L_{iv} graphene becomes an insulator. Intervalley scattering requires that the scattering potential has a Fourier component at a^{-1} with a the lattice spacing. In other words, scattering potential smooth on the scale of lattice spacing does not couple the two valleys of graphene. It turns out the intervalley scattering length in graphene is very large and thus it is of considerable interest to consider what happens in its absence. This is the topic of chapter 6.

Single valley graphene has the same symmetries as a metal with spin-orbit coupling. One might be tempted to conclude that the beta function of these two systems should thus be the same. However, there are several arguments that hint that something completely different is realized. Firstly, consider conductivity at the Dirac point. In the absence of disorder the density of states at the Dirac point is zero and conductance is through evanescent modes. Introduction of disorder will locally change the chemical potential and introduce propagating modes, or in other words disorder will induce a nonzero density of states. Disorder will thus initially increase conductivity. (Another way to think about the same thing is to consider the conductivity enhancement to be due to impurity assisted tunneling [38].) A consequence of this phenomena is that for conductances around the ballistic value the beta function is *positive*.

Secondly, in Refs. 39 and 40 it was shown that the low energy field theory of single valley graphene in the presence of smooth scalar disorder is given in terms of a non-linear sigma model with a topological term. For large conductances the topological term can be neglected and the field theory is the same as for the spin-orbit coupled metal. One thus expects the beta function to approach the limit $1/\pi g$ for $g \gg 1$. We thus have the situation that we have two limits in which the beta function is positive and no theory of how to interpolate between the two limits. One could use the arguments used above expecting the beta function to be monotonous

(which is not always the case, see Fig 1.10) and thus strictly positive. The authors of Ref. 39 gave arguments for a different nonmonotonic scenario in which there is a stable fixed point (as explained in chapter. 6).

In the absence of any analytical tool capable of deciding which beta function is realized, we have developed a numerical method to obtain some evidence for one scenario over the other. In chapter 6 we explain our method and present the results of the numerical simulations. From our results we conclude that the beta function of single valley graphene is strictly positive in contrast to Ref. 39.